Catalysis Today 143 (2009) 309–314

Contents lists available at ScienceDirect

Catalysis Today

journal homepage: www.elsevier.com/locate/cattod

Oxidation of ethane on high specific surface $SmCoO_3$ and $PrCoO_3$ perovskites

M. Alifanti [a], G. Bueno [b], V. Parvulescu [c], V.I. Parvulescu [a], V. Cortés Corberán [b,*]

[a] University of Bucharest, Department of Chemical Technology and Catalysis, B-dul Regina Elisabeta 4-12, Bucharest 030016, Romania
[b] Institute of Catalysis and Petroleumchemistry, CSIC, C. Marie Curie 2, 28049 Madrid, Spain
[c] Romanian Academy, "I. G. Murgulescu" Institute of Physical Chemistry, Splaiul Independentei 202B, Bucharest 060023, Romania

ARTICLE INFO

Article history:
Available online 26 March 2009

Keywords:
Perovskites
Ethane oxidation
Oxidation kinetics
Praseodymium cobalt oxide
Samarium cobalt oxide

ABSTRACT

An adapted sol–gel method allowed synthesizing $SmCoO_3$ and $PrCoO_3$ oxides with high specific surface (ca. 28 $m^2\ g^{-1}$) and a relatively clean perovskite phase at 600 °C, a temperature much lower than the one required in ceramic methods. The perovskites were investigated as catalysts for the oxidation of ethane in the temperature range 300–400 °C. Both catalysts were very active: ethane was activated already at 300 °C, i.e., 100 °C below the temperatures previously reported for perovskites. The main product was CO_2 on both catalysts, but on $PrCoO_3$ oxidehydrogenation (ODH) to ethylene was observed already at 300 °C, with the low selectivity. Even so, this was quite unusual for simple perovskites, and for such a low temperature. TPR data showed that praseodymium decreases the reducibility of Co^{3+} in the perovskite, what could explain the observed ODH, and suggest it proceeds via a Mars–van Krevelen mechanism. Kinetic study showed a similar apparent activation energy for both catalysts (ca. 80 kJ/mol), but a difference in the nature of the participating oxygen species: while on $PrCoO_3$ both adsorbed and lattice species contribute to the reaction, on $SmCoO_3$ contribution of adsorbed species is practically negligible, due to its very high oxygen lability. The results show that these simple perovskites may be promising catalysts for ethane oxidation at relatively low temperatures.

1. Introduction

Perovskite-type oxides are materials of permanent interest due to their tunable oxidative features as, by a proper choice of the cations and a suitable synthesis method, its oxygen content and availability may be varied, while the cubic perovskite structure is preserved. They are quite active in catalytic oxidation, but its use often faces the problem of relatively low surface areas, depending of the preparation method [1]. Among the number of methods reported for the synthesis of perovskites, the choice of a particular one depends mostly on the expected use for these oxides. Application of perovskites in the field of catalysis requires solids with well-developed surface area and porous system. In special, the use of rare-earth-based perovskites for catalytic combustion purposes encounters the difficulty of obtaining high surface area materials, as usually high calcination temperatures are needed for completing the formation of the perovskite structure. Hence, the preparative route plays a critical role on the physical and chemical properties of the reaction products, controlling the structure, morphology, grain size and the surface area of the obtained materials.

Several alternative methods have been reported in the literature to obtain high surface area oxides at relatively low temperatures, many of them using organic compounds and precursors which are decomposed during the calcination. They include the use of precursors prepared via sol–gel [2] spray drying [3], freeze drying [4], heteronuclear complexes [4], combustion of solutions [5] or polymers [6], decomposition of citratres [7] or oxalates [8], among others.

In the sol–gel method, inorganic polymers generated in a first step are further decomposed to give either simple metal oxides, mixed oxides or solid solutions of high homogeneity. This method allows a strict control of composition; at the same time a calcination temperature lower than for the other methods is needed to obtain the desired structure, thus avoiding the sintering phenomena [2]. Sol–gel procedures guarantee stoichiometry and homogeneity of cation distribution. Different complexation agents (oxalic acid [9,10], glycine [11], citric acid [12–16], etc.) have been reported for sol–gel preparation of perovskites.

Ethane is the second most abundant component of natural gas (1.8–5 mol%), and one of the less reactive alkanes. Its main petrochemical use is its conversion to ethylene via steam cracking, an energy-intensive process that gives a complex mixture of hydrocarbons. However, main uses of ethylene require a high purity raw material. The oxidative dehydrogenation (ODH) of ethane could to be a more economic alternative route, but a process for the direct

* Corresponding author. Tel.: +34 915854783; fax: +34 915854760.
E-mail address: vcortes@icp.csic.es (V. Cortés Corberán).

0920-5861/$ – see front matter © 2009 Elsevier B.V. All rights reserved.
doi:10.1016/j.cattod.2009.02.026

transformation of ethane to ethylene is still an unresolved challenge. As a consequence, the main current use of ethane is as a fuel for providing heat to refinery processes. Catalytic combustion could improve the efficiency of non-catalytic burning and decrease the costs of materials for the furnaces, as it proceeds at much lower temperatures. Cobalt containing perovskites, simple or preferably partially substituted, are among the best performing non-metallic catalysts for alkane combustion, and the most studied are those with lanthanum in the A position, being methane oxidation the most studied reaction [1,17].

Much less attention has been devoted to ethane oxidation over perovskites [18–23]. Previous studies pointed to Mn-based perovskites as promising catalysts for ethane ODH [21]. More complex $La_{1-x}Sr_xFeO_3$ perovskite oxides were reported to be active in this reaction at temperatures higher than 400 °C with a maximum in selectivity in ethene at ca. 650 °C, that was always below 40% [22,23]. Also the substitution of La by K in $La_{1-x}K_xMnO_3$ perovskites decreases the activity for ethane combustion and allows the formation of ethylene [18,19]. These findings point out that also the bulkier cation in the A position perovskite structure plays a role in determining the catalytic performance.

All these facts motivated the present paper, where we have studied simple $PrCoO_3$ and $SmCoO_3$ perovskite-type materials with high surface area, prepared via an adapted sol–gel route, their use as catalysts for ethane oxidation, and the kinetics of this reaction. Differences were found in the products distribution on both perovskites, as ethylene was formed on $PrCoO_3$ at temperatures much lower than those previously reported over other, more complex, perovskites. This will be discussed in terms of the effect of cation in the A position.

2. Experimental

The synthesis of $SmCoO_3$ and $PrCoO_3$ perovskites was carried out via an adapted sol–gel route. A 0.5 M ethanolic solution of cobalt nitrate was added dropwise to a 0.5 M ethanolic solution of Ln (Sm or Pr) nitrate until reaching a Ln/Co ratio of 1/1. Ethylene glycol was added to this mixture as complexing agent. Hydrolysis of these complexes was carried out using water, in a molar ratio Ln^{3+}:H_2O = 1:84. The gelification was made at room temperature under a pressure of 10^{-4} atm.

The catalysts precursors were dried at 60 °C under vacuum, and then calcined in air at 600 °C. The chemical analysis (Fe, Co, Cu, Na) of the perovskites and the residual impurities was performed by inductively coupled plasma atomic emission spectrometry using using a PerkinElmer Optima 3000 DV ICP-AES. Prior to each analysis, an exact amount of sample was digested in 10% HCl solution at 90 °C overnight in a teflon lined autoclave.

BET specific surface areas (SSA) were determined by nitrogen adsorption at the temperature of liquid nitrogen on a fully computerized Tri-Star Micromeritics instrument. The catalyst powder was outgassed 12 h at 140 °C under a pressure of 0.1 Pa before each analysis.

XRD patterns of powder samples were recorded using a Seifert 3000 diffractometer. Data were acquired in the 2θ range 10–85° at a 0.02° scan step. SEM measurements were performed on a Hitachi S3000N scanning electron microscope, equipped with a Horiba electron microprobe. XPS spectra were recorded at room temperature at a maximum pressure of 10^{-7} Pa with a Leybold Heraeus spectrometer using monochromatized Al Kα radiation ($h\nu$ = 1486.6 eV). The spectrometer energy scale was calibrated using the Au $4f_{7/2}$ peak (binding energy: 84.0 eV). Charge correction was made considering the C 1s signal of contaminating carbon (C–C or C–H bonds) at 284.8 eV.

Temperature-programmed reduction measurements were conducted on a Micromeritics, AutoChemII apparatus. 0.35 mg samples were introduced in a quartz reactor and were pretreated at 350 °C (in an air flow of 30 mL/min for 1 h and then cooled to room temperature in argon gas flow before reduction was performed. A hydrogen–argon mixture (10% H_2), dried over molecular sieves 5A, was used to reduce the samples at a flow rate of 20 mL/min. Temperature was linearly raised at a rate of 10 °C/min up to 800 °C.

Tests of catalytic oxidation of ethane were done at near atmospheric pressure using mixtures C_2H_6/O_2/He with 3.2–8 mol% C_2H_6, 4–12 mol% O_2 and He balance, in the temperature range 300–400 °C. In all experiments the same ratio W/F = 38.3 g h mol^{-1} C_2 was used.

Reactants and products were analyzed on line in a Varian 4300CX gas chromatograph, equipped with Porapak Q and molecular sieve packed columns and a TCD. All C balances were within 100 ± 3%. Kinetics of the reaction was studied by calculating both ethane ($r_{C_2H_6}$) and (r_{O_2}) conversion rates by the initial rates method in tests where ethane conversion was always kept below 10%. No occurrence of homogeneous transformation of ethane was observed in the range of temperature studied.

3. Results and discussion

3.1. Catalyst characterization

BET measurements carried out for these samples produced surface areas of about 28 m^2 g^{-1} for both catalysts, which is pretty high for Co-based perovskites [3,24]. XRD patterns (Fig. 1) confirmed the formation of the cubic perovskite phase for both formulations. The small reflection of Pr and Sm oxide located around 2θ = 28° could account for an incomplete formation of perovskite phase. However, no reflection associated to Co oxide was detected. This can be interpreted as due to either: (a) an overlapping of the most intense reflections of Co_3O_4 with the perovskite lines at 2θ = 23°, 37° and 45°, (b) to the formation of a non-stoichiometric (Co-enriched) perovskite, or (c) more likely, to an incomplete reaction between the precursors. However, the first supposition can be excluded since XPS showed the existence of only one Co species with the binding energy of the Co 2p3/2 level located at 780.2 eV, which is typical for the perovskite structure [25]. Although the formation of Co-based perovskites requires a lower calcination temperature than those containing other transition metal cations, both the A-site cation and the preparation method may influence the solid–solid reaction. An additional argument in favour of a stoichiometric perovskite composition was provided by the chemical analysis of the calcined materials. ICP-AES analysis indicated a composition corresponding to 50.8 wt% Pr and 21.2 wt% Co for $PrCoO_3$ perovskite, and to 53.9 wt% Sm and 21.3 wt% Co for $SmCoO_3$ perovskite. Actually this corresponds to a 1:1 Ln-to-Co ratio for both perovskites.

The relative high surface areas might indicate a porous structure of the perovskite. Indeed, SEM pictures of the both investigated materials showed a morphology with void spaces, especially in the case of $SmCoO_3$ (Fig. 2). The perovskite structure is usually a compact one, the main reason being the high temperature needed for completing the solid–solid reactions among the various oxide phases. Besides high energy milling procedure, which produces high surface area perovskites by a mechanical approach, the sol–gel method based on complexation with citric acid followed by the corresponding citrates decomposition [24] remains the most common method for synthesis of perovskites with high surface area. The high amount of gases generated during the precursor decomposition leads to a porous material. In our case, the use of ethylene glycol as complexation agent appears to have a similar effect to citric acid.

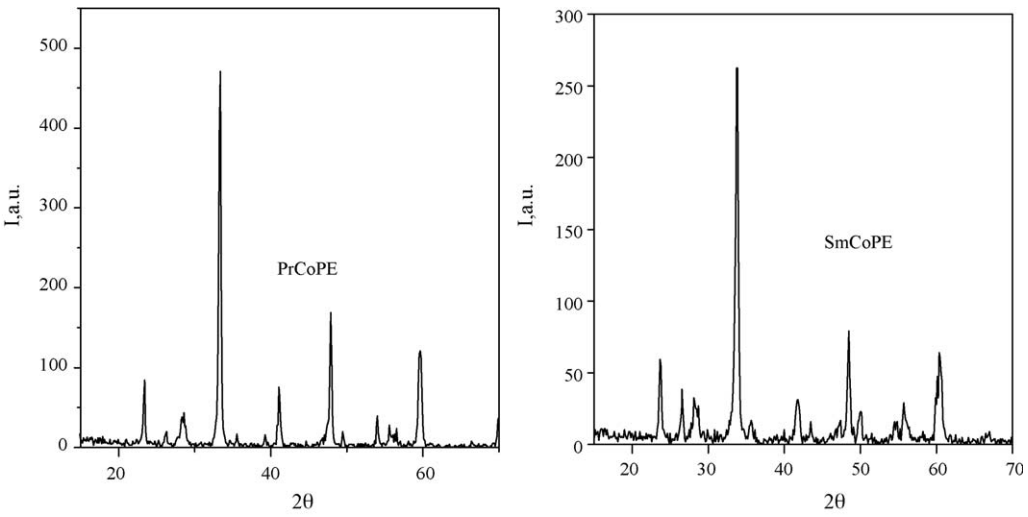

Fig. 1. XRD patterns of $PrCoO_3$ and $SmCoO_3$ samples after calcination at 600 °C.

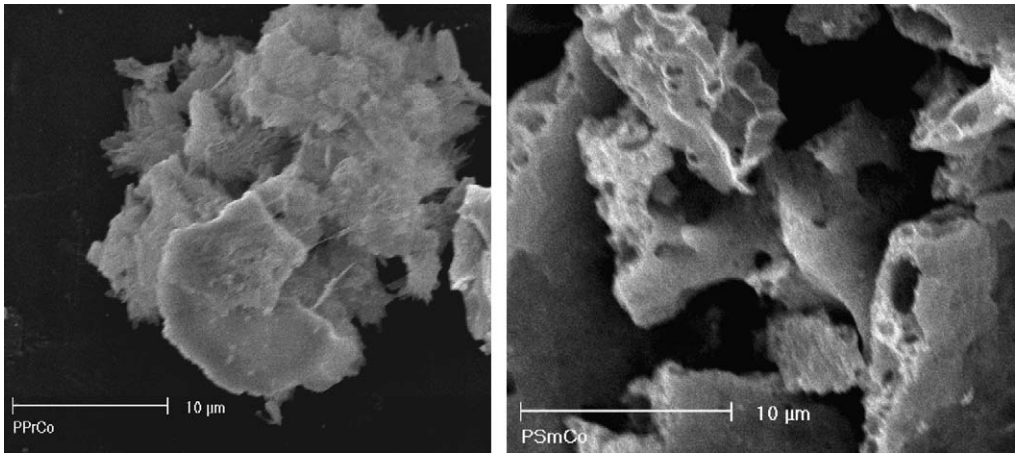

Fig. 2. SEM images of $PrCoO_3$ and $SmCoO_3$ perovskites after calcination at 600 °C.

3.2. Catalytic activity

In the reaction conditions used, $SmCoO_3$ showed a slightly higher specific activity than $PrCoO_3$, the differences never exceeding 20%. Ethane was activated already at 300 °C (ca. 1 mol% conversion), the main products being CO_2 and water, while C_2H_4 and CO were also found in some experiments. This indicates the occurrence of at least three oxidation reactions:

$$C_2H_6 + 7/2O_2 \rightarrow 2CO_2 + 3H_2O \quad (1)$$

$$C_2H_6 + 5/2O_2 \rightarrow 2CO + 3H_2O \quad (2)$$

$$C_2H_6 + 1/2O_2 \rightarrow C_2H_4 + H_2O \quad (3)$$

Although, in principle, the complete oxidation of formed ethylene cannot be discarded:

$$C_2H_4 + 3O_2 \rightarrow 2CO_2 + 2H_2O \quad (4)$$

As conversion was kept very low, the latter reaction was not considered in the kinetic analysis, and the catalytic activity results will be discussed in terms of total combustion and/or oxidative dehydrogenation of ethane.

Perovskites are known as catalysts leading preferentially to total oxidation products due to their high oxygen mobility and the capacity of accommodation of oxygen vacancies [1]. Under the same reaction conditions, $SmCoO_3$ showed a slightly higher specific activity than $PrCoO_3$, the differences never exceeding 20%. The oxidation of ethane on $SmCoO_3$ produced only CO_2 and water, a behaviour characteristic to Co-, Mn-, Fe- and Ni-based perovskites, known to lead to complete oxidation reactions for hydrocarbons even for hydrocarbon-rich reaction mixtures [26]; however, oxidation on $PrCoO_3$ produced also ethylene, the product of oxidehydrogenation (ODH). As expected for this type of materials, CO production is very low, even in the case of reaction mixtures poor in oxygen occurring at relative low temperatures such as 300 °C. Under the conditions used in our study, CO was produced only at 300 °C with oxygen-poor mixtures, i.e., C_2H_6/O_2 = 4/4 and 4/6 (numbers indicate the mol% of each reactant in the feed) with a pretty low selectivity (~1.5%). At 325 °C CO selectivity decreased one order of magnitude. This indicates that Co-based perovskites are able to fully oxidize ethane at quite low temperatures. However, at temperatures around 300 °C it appears that catalysts are not able to supply enough oxygen from the bulk to fully oxidize the hydrocarbon. Arai et al. [27] analyzed the kinetics of hydrocarbon combustion on perovskite catalysts, and concluded that two kinds of oxygen species (adsorbed oxygen and lattice oxygen) may take part in the reaction, which proceeds through two mechanisms. At low temperatures, adsorbed oxygen species would be more active and the kinetics would follow a Rideal-Eley mechanism (suprafacial oxidation); when reaction

temperature is arisen, the coverage of adsorbed oxygen decreases while the reactivity of lattice oxygen increases, giving as a consequence that high temperature combustion is dominantly operated by lattice oxygen (intrafacial mechanism). The latter can be seen as a Mars–van Krevelen mechanism with a much faster reoxidation step. Then, incomplete oxidation to CO at the lowest temperature can be related to the absence, or very limited contribution of suprafacial oxidation mechanism, namely, the lack of sufficient adsorbed oxygen active species. As the temperature increased, the intrafacial mechanism, provides additional oxygen from the bulk to complete total oxidation reactions.

The striking feature of the catalytic behaviour of $PrCoO_3$ is the formation of ethylene at such a low temperature (300 °C), and observed in the whole temperature range. The effect of reactants partial pressures on ethane conversion and ethylene selectivity was studied at various temperatures (Figs. 3 and 4). When the oxygen content in the feed is 8 mol%, within the limits of the experimental error, there is practically no variation of ethylene selectivity (the balance being CO_2) in the whole range of temperatures and ethane partial pressures (Fig. 3), pointing to similar activation routes for both ODH and combustion. Fig. 4 shows higher ethylene selectivities for low O_2 partial pressures indicating that ethane is not thermally but catalytically activated.

Looking comparatively to $PrCoO_3$ and $SmCoO_3$, the higher oxidative capacity of the latter may be linked to a higher reducibility. Indeed, in the lanthanide series perovskite reducibility decreased as the Goldschmidt factor (tolerance factor, t) increased [28]. The H_2-TPR profiles recorded for $SmCO_3$ and $PrCoO_3$ (Fig. 5) confirm such a behaviour. Both the reduction of Co^{3+} to Co^{2+} and of Co^{2+} to Co^0 occur at lower temperatures for $SmCoO_3$ than for $PrCoO_3$. This behaviour should be related on the stabilities of Ln(3+)/(2+) states. Based on in situ Mossbauer experiments we have recently demonstrated that the lanthanide species is not just a spectator, but its oxidation state changes also during the oxidation process [25]. The assignment of consumption peaks is in agreement with the literature data [28]. It should be noted that, as samples were pretreated at 350 °C prior to the tests, differences revealed in the TPR-profiles are due exclusively to lattice oxygen in the perovskites. Therefore, one may infer that the occurrence of oxidative dehydrogenation over $PrCoO_3$ and its absence over $SmCoO_3$ are due to their different reducibility, and that the ethane ODH over the former follows a Mars–van Krevelen mechanism, where lattice oxygen from $PrCoO_3$ is consumed.

Catalysts reported for ethane ODH include both metals and oxides. The best ones are those based on Pt, either utilizing very

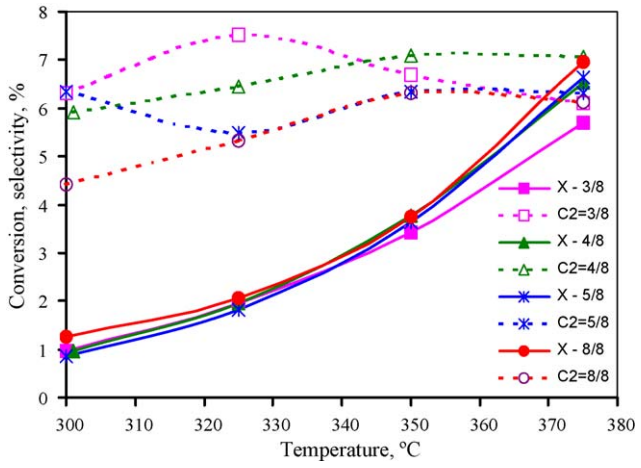

Fig. 3. Influence of temperature and C_2H_6 partial pressure on ethane conversion (X, continuous lines) and ethylene selectivity (C_2=, dotted lines) in ethane oxidation on $PrCoO_3$. Fractions indicate the C_2H_6/O_2 mol% ratio in the feed.

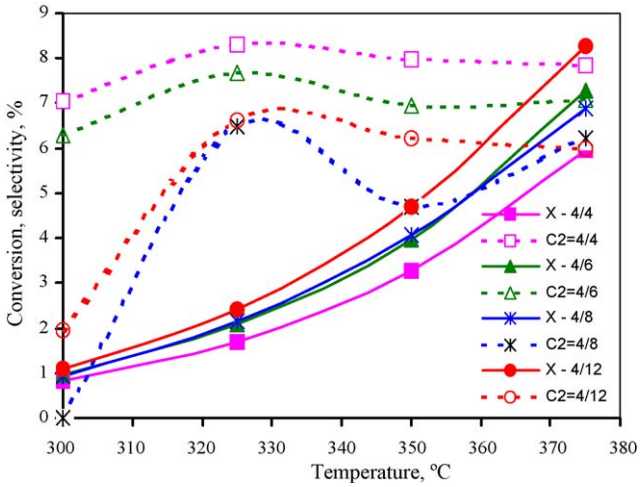

Fig. 4. Influence of temperature and O_2 partial pressure on ethane conversion (X, continuous lines) and ethylene selectivity (C_2=, dotted lines) in ethane oxidation on $PrCoO_3$. Fractions indicate the C_2H_6/O_2 mol% ratio in the feed.

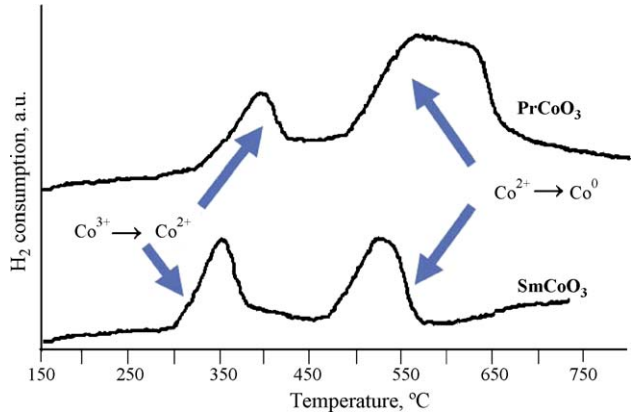

Fig. 5. Temperature-programmed reduction profiles of $PrCoO_3$ and $SmCoO_3$ (10% H_2 flow, heating rate 10 °C/min).

short contact times and high temperatures [29], or improved with Sn or Cu as dopants [30,31]. Several types of oxides have also been studied, but for high conversion levels the complete oxidation reactions (of both the reactant, ethane, and desired product, ethylene) cannot be avoided [29,32–35]. Among them, Heracleous and Lemonidou [36] reported excellent catalytic features of a Ni–Nb mixed oxide. Their detailed kinetic study [37] shows that ethane ODH proceeds via a Mars–van Krevelen mechanism in which the O^{2-} species are the selective catalytic sites while O^- species accommodated at the surface are the non-selective ones.

Concerning perovskites, ethane oxidation over pure and Ca-, Mg-, Sr-, La-, Nd-, and Y-substituted $BaCeO_3$ perovskites under oxygen limited conditions produced ODH at temperatures above 650 °C, but at the cost of structural stability [20]; below that temperature, only total combustion was observed. Also complex $La_{1-x}Sr_xFeO_3$ oxides were reported to be active in ODH at temperatures higher than 400 °C, with a maximum in ethylene selectivity (always below 40%) around 650 °C [22,23]. Some studies pointed to Mn-based perovskites as promising catalysts for ethane ODH [21]. Ethylene selectivity on $PrCoO_3$ in the present study was comparable to the values observed on K-substituted La–Mn perovskites [18,19]. In that case, selectivity to ethylene at isoconversion increased with the increase of potassium content, which was interpreted as due to a change in the mobility of oxygen species: progressive substitution of La^{3+} by K^+ decreased the number of oxygen vacancies, thus reducing oxygen mobility. This

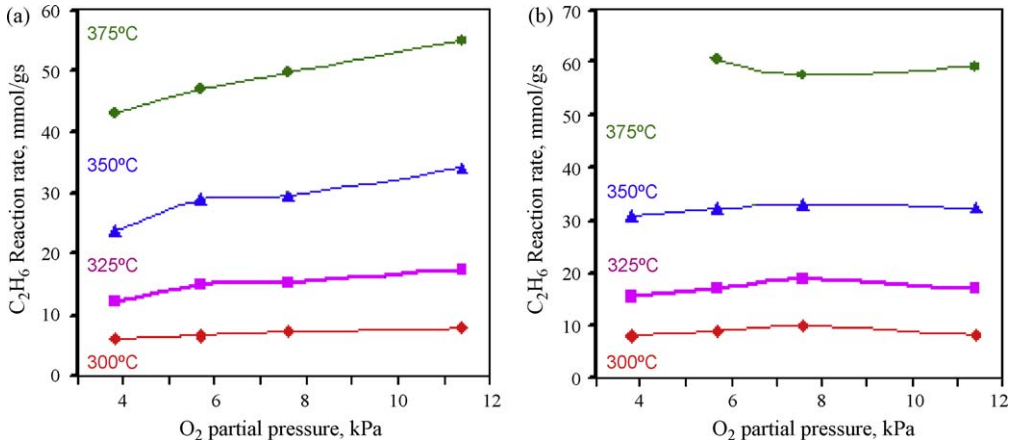

Fig. 6. Influence of oxygen partial pressure on ethane consumption rate at various temperatures on: (a) $PrCoO_3$ and (b) $SmCoO_3$.

seems to support our interpretation that ODH observed over $PrCoO_3$ is due to its lower oxygen mobility and/or reducibility.

3.3. Kinetic study

Ethane and oxygen consumption rates on both catalysts were evaluated in the whole range of experimental conditions. As expected, ethane consumption rates increased with temperature, but at a given temperature they do not vary drastically (Fig. 6). On the other hand, the increase of the oxygen partial pressure while ethane concentration is kept constant leads to a slight but constant increase of the reaction rate. On $PrCoO_3$ (Fig. 6a) the reaction rate of ethane increases with the oxygen partial pressure. This variation is steeper in the low partial pressures range. In the case of $SmCoO_3$ the ethane consumption rate at each temperature is constant for the whole range of oxygen partial pressure, pointing to deep oxidation abilities of this catalyst.

For the kinetic analysis, the conversion of ethane was kept in all the experiments below 10%, and, as a first approach, a simple power-law model: $r_{C_2H_6} = k\, p_{C_2H_6}{}^m\, p_{O_2}{}^n$ was applied. Though power-law model does not provide deep information on the reaction mechanism, it is a very rapid method for establishing some parameters useful in chemical engineering. With this respect, considering that only CO_2 and C_2H_4 are formed, the parameters listed in Table 1 were derived by the method of varying ethane or oxygen partial pressure, each at one time, while keeping constant the other. Apparent activation energy was practically equal for both catalysts, ca. 80 kJ/mol. This value is practically equal to that found for ethane oxidation over K-substituted La–Mn perovskites, 77 kJ/mol [18,19]. The reaction orders for ethane and oxygen are similar and rather low for $PrCoO_3$, that catalyzes ODH; in contrast to $SmCoO_3$, for which reaction order in ethane is higher.

Arai et al. [27] analyzed the kinetics of hydrocarbon combustion on perovskite catalysts according to the description mentioned above, that leads to the rate expression:

$$r_{C_2H_6} = \frac{k_a\, p_{C_2H_6} (K_{O_2}\, p_{O_2})^{1/2}}{[1 + (K_{O_2}\, p_{O_2})^{1/2}]} + k_1\, p_{C_2H_6} \quad (5)$$

Table 1
Power-law derived kinetic parameters for ethane oxidation on $PrCoO_3$ and $SmCoO_3$.

Catalyst	E_a[a] (kJ/mol)	m[b]	n[b]
$PrCoO_3$	75 ± 10	0.25 ± 0.02	0.30 ± 0.02
$SmCoO_3$	82 ± 5	0.52 ± 0.03	0.23 ± 0.02

[a] Apparent activation energy with 95% confidence limits.
[b] At 300 °C.

that if coverage of oxygen is small, i.e., $1 \ll (K_{O_2}\, p_{O_2})^{1/2}$, it becomes:

$$r_{C_2H_6} = k_a\, p_{C_2H_6} (K_{O_2}\, p_{O_2})^{1/2} + k_1\, p_{C_2H_6} \quad (6)$$

This allows to estimate the contribution of each type of oxygen species, by plotting the rate vs. $(p_{O_2})^{1/2}$. The first term represents the contribution of adsorbed oxygen (the higher the plot slope, the higher its contribution) and the second one (the intercept of

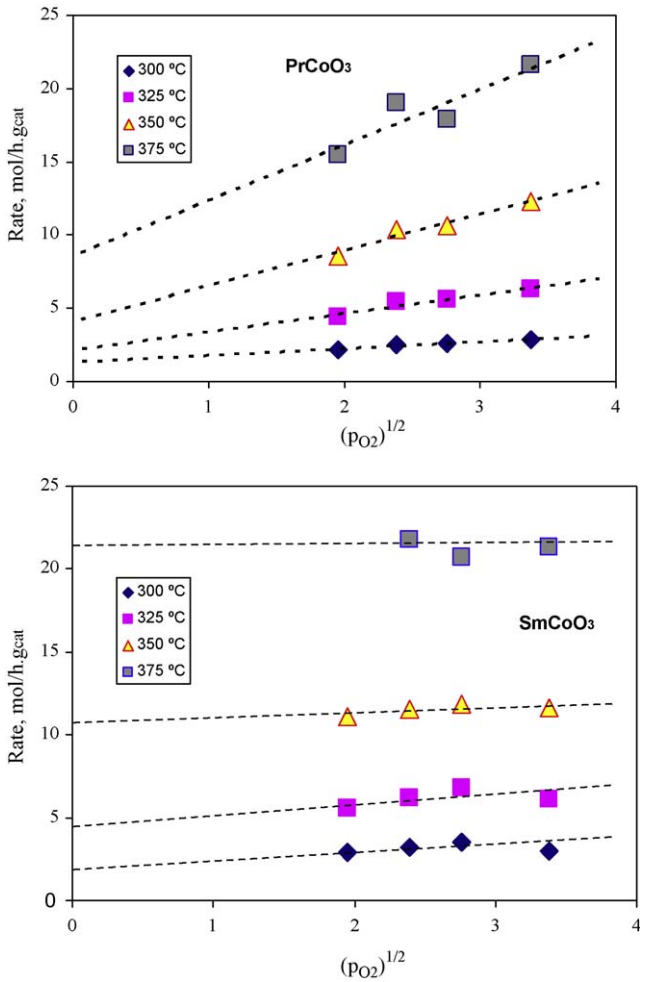

Fig. 7. Plots of ethane consumption rate vs. square root of oxygen partial pressure on $PrCoO_3$ and $SmCoO_3$.

ordinates axis) that of lattice oxygen. Fig. 7 shows such plots for ethane oxidation on both perovskites. It can be seen that on $SmCoO_3$ oxygen comes mostly from lattice (very low slope and high *y*-axis intercept), even at the low temperatures explored here. This can be explained by its very high reducibility, as shown in its H_2-TPR profile. On the contrary, due to its lower reducibility, on $PrCoO_3$ the contribution from lattice oxygen is much lower, and adsorbed oxygen contributes to the overall reaction even at 375 °C. This might be a reason why formation of ethylene, that proceeds with lattice oxygen via a Mars–van Krevelen mechanism, is always low.

An important aspect to be underlined is that, on the contrary to substituted $BaCeO_3$ perovskites, after reaction no structural or morphologic changes were observed, indicating that indeed these perovskites are stable structures at these reaction temperatures. This feature adds to the potentiality of these oxides as promising materials for the low temperature activation of ethane.

4. Conclusions

$SmCoO_3$ and $PrCoO_3$ perovskites were synthesized by an adapted sol–gel method, using ethylene glycol as complexing agent. This procedure allowed the preparation of a relatively clean perovskite phase in both cases at a lower calcination temperature than the one required in ceramic methods. Both oxides were active for the oxidation of ethane in the temperature range of 300–400 °C. Ethane was activated at 300 °C, i.e., 100 °C below the temperatures reported for Ti- or Fe-based perovskites. On $SmCoO_3$ the oxidation was specifically conducted to CO_2 and H_2O, but on $PrCoO_3$ ethylene production, though with a low yield, was observed. Even with low selectivity, the formation of ethylene was surprising for a simple (unsubstituted) perovskite, specially at such low temperatures. Kinetic measurements combined with TPR studies have shown that the oxygen for ODH is provided by the catalyst, a Mars–van Krevelen mechanism being suggested to describe ethylene formation on this perovskite. The comparison of the catalytic performance and reducibility properties of the two perovskites shows that cations in the A position of the perovskite cubic structures (Pr or Sm) clearly play a role in determining the catalytic performance. It is well known that praseodymium can have a variety of oxidation states, what could favour the easy electron transfer to cobalt atoms, who are the active centres for oxidation. This transfer will stabilize Co^{3+} against reduction, thus reducing its oxidating power. As a consequence, total oxidation proceeds with both adsorbed and lattice oxygen, but some activated hydrocarbon molecules are not completely oxidized, leading to the observed formation of ethylene.

In addition, high surface area praseodymium cobalt perovskites prepared by this method may behave as promising catalysts for ethane ODH at relatively low temperatures with further modification of the formulation: previous results reported with K-substituted La–Mn perovskites [18,19] could indicate that a partial substitution of Pr with alkaline or alkaline-earth elements could be a way to improve ODH selectivity.

References

[1] L.G. Tejuca, J.L.G. Fierro, J.M.D. Tascón, Adv. Catal. 36 (1989) 237.
[2] C.D. Chandler, C. Roger, M.J. Hampdon-Smith, Chem. Rev. 93 (1993) 1205.
[3] A. González, E. Martínez Tamayo, A. Beltrán Porter, V. Cortés Corberán, Catal. Today 33 (1997) 361.
[4] C.H. Marcilly, P. Country, B. Delmon, J. Am. Ceram. Soc. 53 (1970) 56.
[5] A.C.F.M. Costa, E. Tortella, M.R. Morelli, M. Kaufman, R.H.G.A. Kiminami, J. Mater. Sci. 37 (2002) 3569.
[6] J. Jiu, Y. Ge, X. Li, L. Nie, Mater. Lett. 54 (2002) 260.
[7] S. Prasad, N.S. Gajbhiye, J. Alloys Compd. 265 (1998) 87.
[8] B.L. Cushing, V.L. Kolesnichenko, C.J. O'Connor, Chem. Rev. 104 (2004) 3893.
[9] R.J. Bell, G.J. Millar, J. Drennan, Solid State Ionics 131 (2000) 211.
[10] V. Uskoković, M. Drofenik, Mater. Des. 28 (2007) 667.
[11] C.H. Jung, D.K. Kim, J. Mater. Synth. Process. 10 (2002) 23.
[12] K.-S. Song, S.-K. Kang, S.D. Kim, Catal. Lett. 49 (1997) 65.
[13] M. Kakihana, T. Okubo, M. Arima, Y. Nakamura, M. Yashima, M. Yoshimura, J. Sol–Gel Sci. Technol. 12 (1998) 95.
[14] A. Majid, J. Tunney, S. Argue, D. Wang, M. Post, J. Margeson, J. Alloys Compd. 398 (2005) 48.
[15] H. Taguchi, S. Yamasaki, M. Nagao, Y. Sato, K. Hirota, O. Yamaguchi, J. Mater. Sci. 41 (2006) 7978.
[16] M. Alifanti, M. Florea, V.I. Pârvulescu, Appl. Catal. B: Environ. 70 (2007) 400.
[17] A. Baiker, P.E. Marti, P. Keusc, E. Fritsch, A. Reller, J. Catal. 146 (1994) 268–276.
[18] Y. Ng Lee, F. Sapina, E. Martinez, J.V. Folgado, V. Cortés Corberán, Stud. Surf. Sci. Catal. 110 (1997) 747.
[19] Y. Ng Lee, Z. El-Fadli, F. Sapiña, E. Martínez-Tamayo, V. Cortés Corberán, Catal. Today 52 (1999) 45.
[20] J.E. Miller, A.G. Sault, D.E. Trudell, T.M. Nenoff, S.G. Thoma, N.B. Jackson, Appl. Catal. A: Gen. 201 (2000) 45.
[21] F. Donsi, R. Pirone, G. Russo, J. Catal. 209 (2002) 51.
[22] G. Yi, T. Hayakawa, A.G. Andersen, K. Suzuki, S. Hamakawa, A.P.E. York, M. Shimizu, K. Takehira, Catal. Lett. 38 (1996) 189.
[23] H.X. Dai, C.F. Ng, C.T. Au, J. Catal. 189 (2000) 52.
[24] N. Tien-Thao, H. Alamdari, S. Kaliaguine, J. Solid State Chem. 181 (2008) 2006.
[25] M. Alifanti, M. Florea, G. Filotti, V. Kuncser, V. Cortes-Corberan, V.I. Parvulescu, Catal. Today 117 (2006) 329.
[26] T. Hayakawa, A.G. Andersen, H. Orita, M. Shimizu, K. Takehira, Catal. Lett. 16 (1992) 373.
[27] H. Arai, T. Yamada, K. Eguchi, T. Seiyama, Appl. Catal. 26 (1986) 265.
[28] L.R. Lago, G. Bini, M.A. Peña, J.L.G. Fierro, J. Catal. 167 (1997) 198.
[29] L.D. Schmidt, M. Huff, S.S. Bharadwaj, Chem. Eng. Sci. 49 (1994) 3981.
[30] P.M. Torniainen, X. Chu, L.D. Schmidt, J. Catal. 146 (1994) 1.
[31] A.S. Bodke, D. Henning, L.D. Schmidt, S.S. Bharadwaj, J.J. Maj, J. Siddall, J. Catal. 191 (2000) 62.
[32] E.M. Kennedy, N.W. Cant, Appl. Catal. 75 (1991) 321.
[33] S.A.R. Mulla, O.V. Buyevskaya, M. Baerns, J. Catal. 197 (2001) 43.
[34] D.W. Flick, M.C. Huff, Appl. Catal. A: Gen. 187 (1999) 13.
[35] A. Beretta, P. Forzatti, J. Catal. 200 (2001) 45.
[36] E. Heracleous, A.A. Lemonidou, J. Catal. 237 (2006) 162.
[37] E. Heracleous, A.A. Lemonidou, J. Catal. 237 (2006) 175.